JOURNAL OF AIRCRAFT
Vol. 42, No. 5, September–October 2005

Semi-Active Vibration Isolation Using Magnetorheological Isolators

Young-Tai Choi* and Norman M. Wereley†
University of Maryland, College Park, Maryland 20742
and
Young-Sik Jeon‡
Yuhan College, Kyungki-Do 422-794, Republic of Korea

An experimental and theoretical analysis of a vibration isolation system that uses magnetorheological (MR) fluid-based semi-active isolators is presented. In doing so, a vibration isolator that uses MR fluids is designed, manufactured, and experimentally evaluated. Typically, a Bingham-plastic model, with its accompanying zero speed force step discontinuity, would be used to model an MR isolator. A new nonlinear model, with simple low-speed hysteresis characteristics, is proposed to describe the hysteresis force characteristics of the MR isolator. The damping forces of the MR isolator with different excitation frequency and current input are measured and compared with that resulting from the hysteresis model for the verification of the theoretical analysis. A vibration isolation system with the MR isolator is constructed, and its dynamic equation of motion is derived. A simple skyhook controller is formulated to attenuate the vibration of the system. Controlled performances of the vibration isolation system are experimentally and theoretically evaluated in the frequency and time domains. A key conclusion is that a simple model of the low-speed force vs low-speed velocity hysteresis characteristics is necessary for successful prediction of open- and closed-loop performance in both the time and frequency domains.

Introduction

AVIONICS and sensitive instruments in aircraft and helicopters work under a high vibratory environment due to engine and transmission vibrations. In particular, military air vehicles are subjected to higher vibration and shock loads due to gunfire and quick maneuvers. To cope with such vibration and shock problems, vibration isolators have been used. Vibration isolators can isolate systems from various sources, so that systems will not be exposed to significant dynamic stress and fatigue damage. There are three types of potential vibration isolators: passive, semi-active, and active. Passive isolators featuring elastomeric materials and/or hydraulic valves/dampers provide design simplicity and cost-effectiveness.[1–3] However, performance is limited because of no controllable damping or stiffness. On the other hand, active isolators featuring electromagnetic,[4] servovalve,[5,6] and piezoceramic[7,8] actuators may provide high control performance over a wide frequency range. However, such active isolators require high-power sources and complex configurations. Recently, to mitigate disadvantages of active isolators, semi-active isolators have been introduced. Among these, we focus on magnetorheological (MR) fluid-based semi-active isolators. MR isolators are known to have advantages such as continuously damping force and fast response. However, MR isolators exhibit nonlinear force hysteresis characteristics dependent on excitation frequency and current input.

The Bingham-plastic model is widely used to evaluate the behavior of MR fluid-based applications because of its simplicity in form. However, the Bingham-plastic model cannot explain the force vs low-speed velocity hysteresis characteristics of MR isolators. Therefore, a nonlinear hysteresis model is needed to capture accurately the force behavior of MR isolators. For theoretical modeling of nonlinear hysteresis characteristics of MR dampers, several studies have been reported.[9–20]

Wereley et al.[9] proposed the hysteretic bivious model composed of several piecewise continuous functions. The hysteretic bivious model captures nonlinear hysteresis characteristics of MR dampers accurately, but its mathematical form is not so simple. They also proposed the nonlinear viscoelastic plastic model[10–12] that is a mechanisms-based model closer to physical phenomena. The nonlinear viscoelastic plastic model has seven parameters associated with preyield mechanisms, postyield mechanisms, and yield force and shows good accuracy in the capture of the hysteresis behavior of the MR damper. Spencer et al.[13] and Dyke et al.[14] presented the Bouc–Wen model for the prediction of the damping force of electrorheological (ER) or MR dampers. The Bouc–Wen model needs 14 parameters to describe the hysteresis characteristics, and its mathematical formulation incorporates strong nonlinear differential equations. Gavin et al.[15] proposed the multivariable curve-fitting model with Chebyshev and Legendre polynomials. The multivariable curve-fitting model shows good ability to predict accurately the force behavior of ER dampers, but its mathematical formulation is too complex. Makris et al.[16] proposed the neural network model to predict the hysteresis characteristics of ER dampers. The neural network model is combined with the phenomenological model such as the BingMax model and shows favorable accuracy in the prediction of the hysteresis response of ER dampers. However, the neural network model inherently requires somewhat iterative computational calculation for training. Sims et al.[17,18] constructed the spring-mass-damper model for the prediction of the hysteresis behavior of ER dampers. The spring-mass-damper model physically accounts for the dynamic behavior of the damper, but requires more or less complicated numerical techniques to solve the implicit motion equations. Choi et al.[19] reported the polynomial model that is a sixth-order polynomial function with seven coefficients. These coefficients of the polynomial function were identified along with two regions: negative and positive accelerations. The polynomial model captures the hysteresis behavior of ER dampers accurately, but its mathematical form is a little complex. Hong et al. proposed the hydromechanical model[20] that is derived from the lumped hydraulic

Received 28 January 2004; accepted for publication 4 February 2004.

*Research Associate, Smart Structures Laboratory, Department of Aerospace Engineering.
†Associate Professor, Smart Structures Laboratory, Department of Aerospace Engineering.
‡Professor, Department of Tool and Mold Design.

components of the ER damper. The hydromechanical model consists of physically motivated simple parameters such as inertia, damping, yield force, and compliance associated with ER or MR dampers, but utilizes a second-order nonlinear differential equation. The hydromechanical model shows good accuracy in the prediction of the hysteresis characteristics.

These hysteresis models reviewed here can successfully represent the hysteresis characteristics of ER or MR dampers. However, these models are difficult to apply directly to control applications because they are relatively complex as compared to the Bingham-plastic model, and the hysteresis parameters are not directly correlated with control current input. Consequently, the main contributions of this paper are 1) to propose a nonlinear hysteresis MR isolator model having simplicity and nominal accuracy and 2) to study its impact on the performance predictions of MR isolators in open- and closed-loop measurements in both time and frequency domains. This is done in comparison to the Bingham-plastic model.

In this study, a vibration isolation system that uses MR fluid-based semi-active isolators is investigated through experimental and theoretical works. An MR fluid-based vibration isolator used to cope with the vibration isolation problem of avionic packages is designed, manufactured, and tested in a single-degree-of-freedom (SDOF) mount. A new nonlinear hysteresis model with simplicity in form is proposed to describe the low-speed hysteresis force characteristics of the MR isolator. The damping forces of the MR isolator with different excitation frequency and current input are measured and compared with that resulting from the hysteresis model for the verification of the theoretical analysis. A vibration isolation system with the MR isolator is then constructed, and its dynamic equation of motion is derived. From the equation, a simple skyhook controller[21] is formulated to attenuate the vibration of the system. Closed-loop control performance of the vibration isolation system under constant current input and simple skyhook controller are experimentally and theoretically evaluated in the frequency and time domains for both the Bingham-plastic model and the nonlinear hysteresis model.

MR Vibration Isolators

MR isolators produce a variable damping force in response to magnetic fields proportional to applied current input. The magnitude of the damping force can be continuously controlled by variation of the current input. Therefore, MR isolators have additional advantages, such as simple mechanical configuration, other than continuous force control ability and fast response. The schematic diagram of an MR isolator designed and manufactured in this study is shown in Fig. 1. This MR isolator was designed to have the damping level appropriate to cope with the vibration isolation problem of avionics packages. To have a lightweight isolator, most components of the isolator were manufactured from aluminum, except for the magnetic activation areas. In addition, the size of the MR isolator is compact: 79 mm in height and 69 mm in outer diameter. A photograph of the MR isolator is shown in Fig. 2.

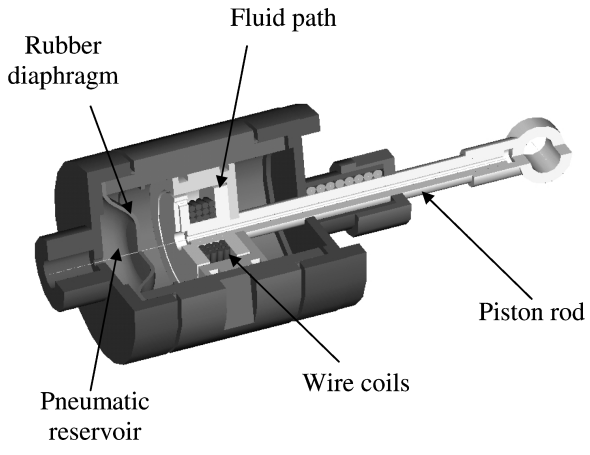

Fig. 1 Schematic diagram of MR isolator.

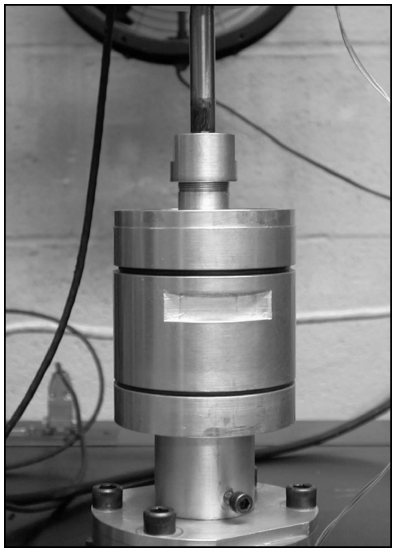

a)

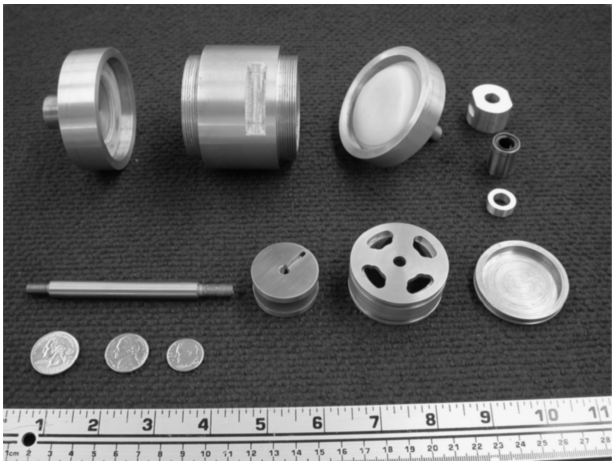

b)

Fig. 2 Photograph of MR isolator: a) assembly and b) components.

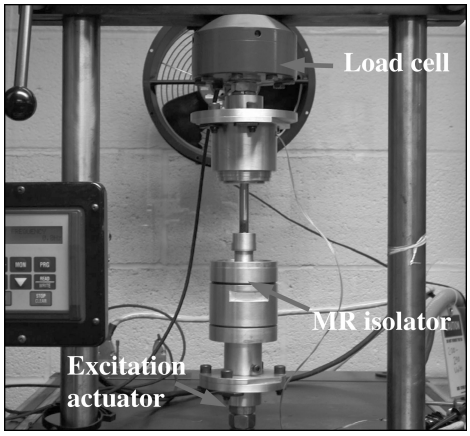

Fig. 3 Experimental setup for damping force test of MR isolator.

Damping Force Test

For the damping force test of the MR isolator, an experimental setup is constructed as shown in Fig. 3. The MR isolator is placed between the load cell and excitation actuator. The load cell is fixed, and the bottom part of the MR isolator is moved through the excitation actuator. In the absence of current input, the MR isolator just produces passive damping forces due to fluid viscosity and seal friction. However, on application of current input to the MR isolator, the MR isolator produces an additional damping force due to the yield

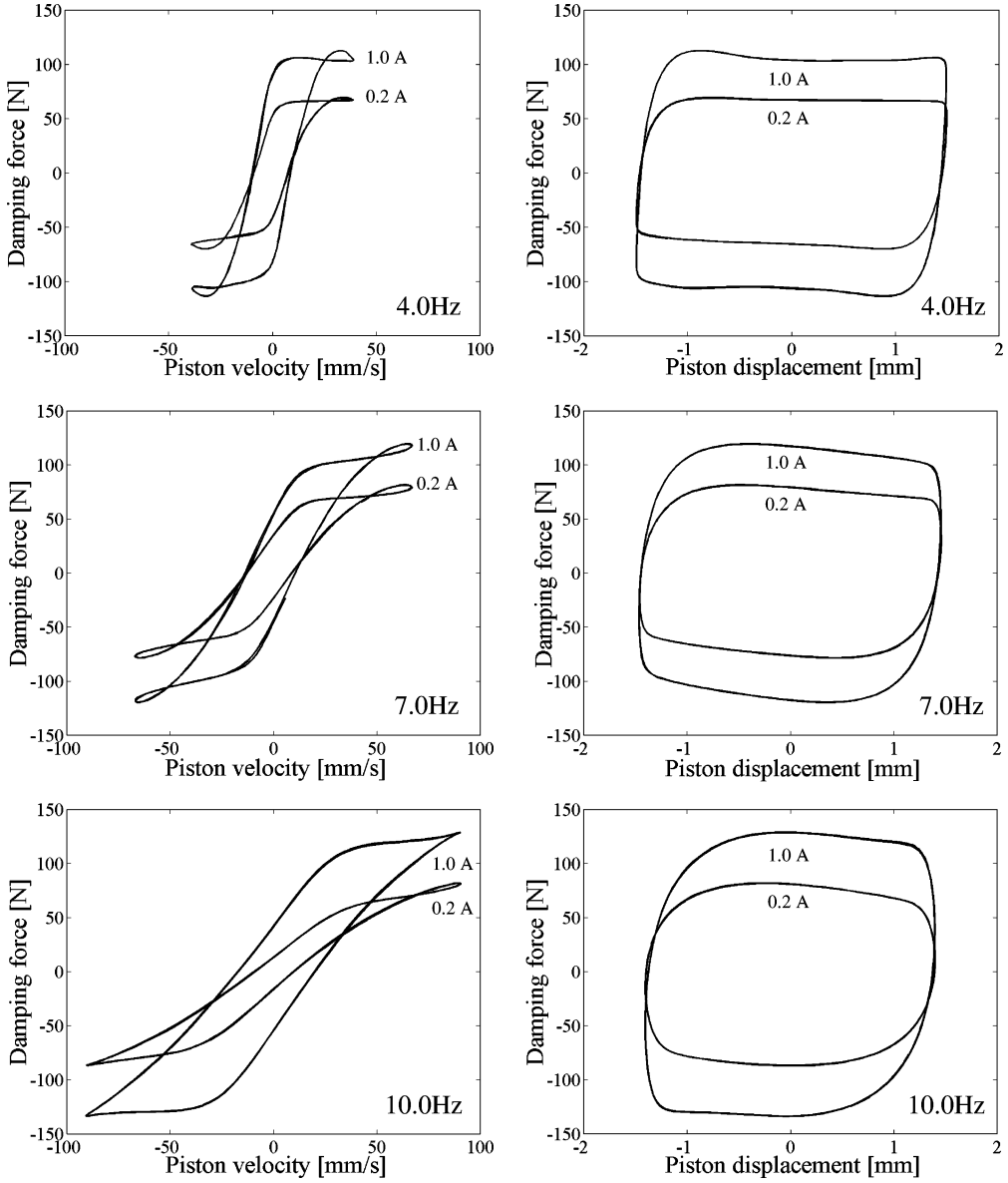

Fig. 4 Experimental results of the MR isolator under different sinusoidal excitations: a) force vs velocity and b) force vs displacement.

stress of the MR fluid. The additional damping force can be continuously controlled according to the applied current input. In this study, the excitation input used is a sinusoidal excitation with constant displacement amplitude and single excitation frequency. In addition, in the case of the vibration isolation of the avionics package, the displacement amplitude of the excitation was nominally as small as 1–2 mm. In this study, the displacement amplitude is 1.3 mm.

The experimental results of the MR isolator are shown in Fig. 4. The force vs velocity and the force vs displacement plots show excitation frequencies of 4.0, 7.0, and 10.0 Hz at different current inputs of 0.2 and 1.0 A. As observed from the force vs velocity plot in Fig. 4a, the MR isolator shows a hysteresis loop, and its shape varies according to the excitation frequency and the applied current input. In particular, the slope of the hysteresis loop goes down as the excitation frequency increases, but goes up as the applied current input increases. This is because the yield stress of the MR fluid weakens at relatively high excitation frequency[22] and because MR fluids produce the yield stress closer to Coulomb friction at relatively high current input. On the other hand, the shape of the force vs displacement hysteresis cycle at an excitation of 4 Hz is close to a rectangular, as shown in Fig. 4b, but, as the excitation increases, the shape becomes close to a circle. This is a result of the fact that the slope of the hysteresis loop in the force vs velocity plot decreases.

Theoretical Modeling

We will consider two theoretical models: 1) a Bingham-plastic model that ignores the preyield compression loop and 2) a nonlinear hysteresis model. When the Bingham-plastic model[23–25] is used, the damping force of the MR isolator can be expressed as follows:

$$f_d = c\dot{x}_e + kx_e + (f_y + f_f)\,\mathrm{sgn}(\dot{x}_e) \tag{1}$$

Here, f_d is the damping force of the MR isolator, c is the viscous damping, k is the stiffness due to gas, f_f is the seal friction force, and f_y is the yield force due to MR fluids of which magnitude is exponentially proportional to applied current input. In addition, x_e is the excitation displacement and sgn$(\cdot)$ is the signum function. The typical behavior of the Bingham-plastic model in force vs piston velocity plot is shown schematically in Fig. 5a.

The damping force of the MR isolator can be also expressed by means of a new nonlinear hysteresis model proposed in this study, as follows:

$$f_d = c\dot{x}_e + kx_e + (f_y + f_f)\tanh[(\dot{x}_e + \lambda_1 x_e)\lambda_2] \tag{2}$$

Here, tanh$[\cdot]$ is the hypertangent function and λ_1 and λ_2 are characteristic parameters of the nonlinear hysteresis model used to capture

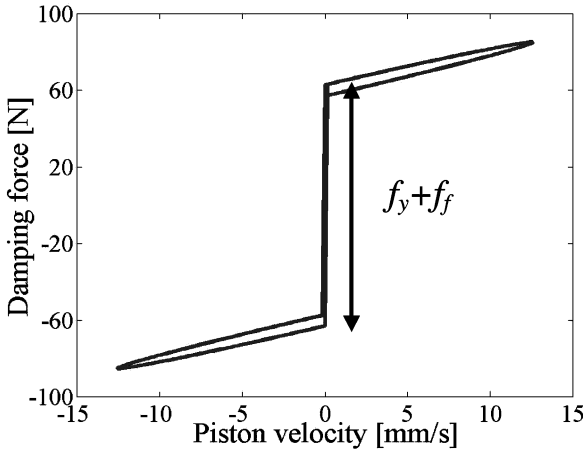

a)

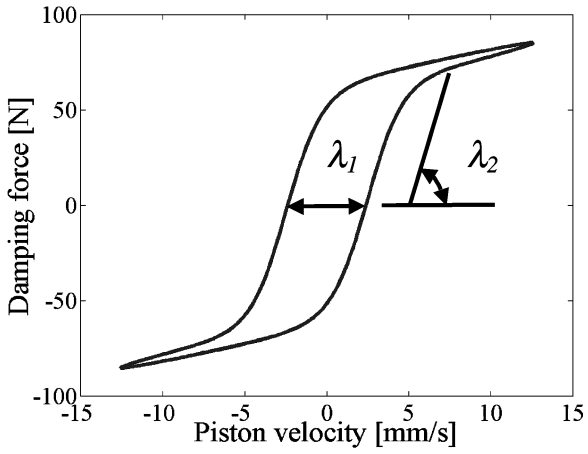

b)

Fig. 5 Typical behavior of theoretical models in force vs piston velocity plot: a) Bingham-plastic model and b) nonlinear hysteresis model.

the hysteresis loop. The parameter λ_1 accounts for the width of the hysteresis loop in force vs piston velocity, and λ_2 accounts for the slope of the hysteresis loop (Fig. 5b). Note that the larger the parameter λ_2, the steeper the slope of the hysteresis loop. To establish the hysteresis model structure, the parameters λ_1 and λ_2 are identified by a curve-fitting method. The identified parameters are plotted over a range of excitation frequency and constant current input, in Fig. 6. From Fig. 6, the parameters λ_1 and λ_2 are strong functions of excitation frequency, but weak functions of current input.

Experimental Verifications

Figure 7 presents the damping force vs piston velocity of the MR isolator. In Fig. 7, the solid line stands for experimental data and dashed line is theoretical data. The data were collected at the conditions such as an excitation frequency of 5.5 Hz and a constant current input of 0.4 A. Note that the Bingham-plastic model cannot capture hysteresis behavior of the MR isolator. However, the nonlinear hysteresis model proposed in this study captures the behavior relatively well. Note that even though the Bingham-plastic model cannot capture the hysteresis loop, it can still predict the magnitude of the damping force. Because of this, the Bingham-plastic model could be widely used in basic performance predictions of ER/MR applications.

Figure 8 presents the damping force vs piston velocity at an excitation frequency of 8.5 Hz and constant current inputs of 0.2 and 1.0 A. As shown in Fig. 8, the nonlinear hysteresis model also captures the behavior of the MR isolator at different conditions well. Similar results are obtained at the damping force vs piston displacement shown in Fig. 9. Therefore, these results show that the nonlinear

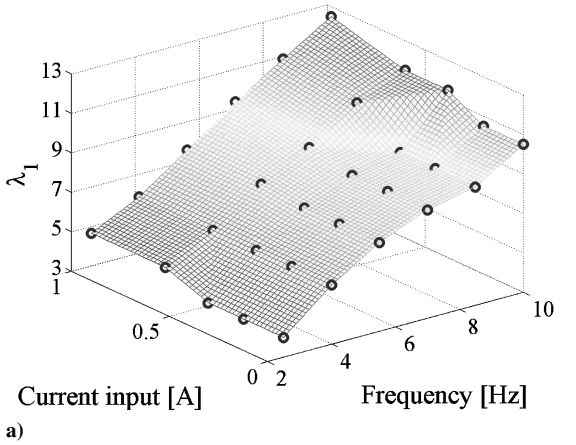

a)

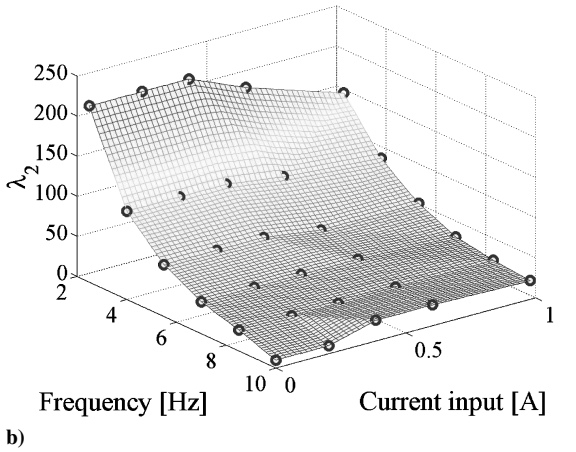

b)

Fig. 6 Identified parameters of the nonlinear hysteresis model: a) parameter λ_1 and b) parameter λ_2.

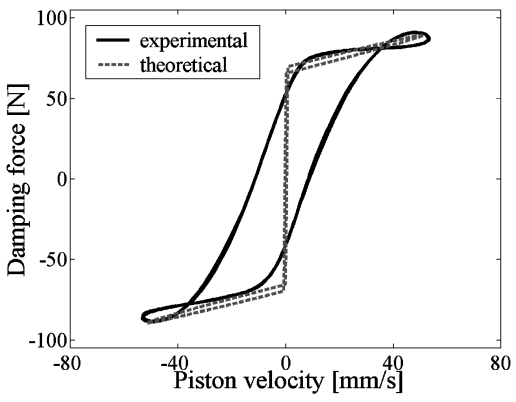

a)

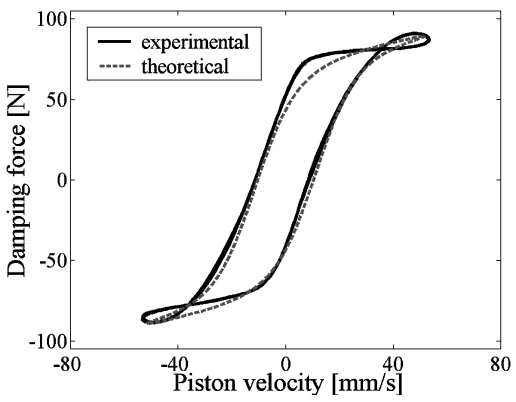

b)

Fig. 7 Damping force vs piston velocity (0.4 A at 5.5 Hz): a) Bingham-plastic model and b) nonlinear hysteresis model.

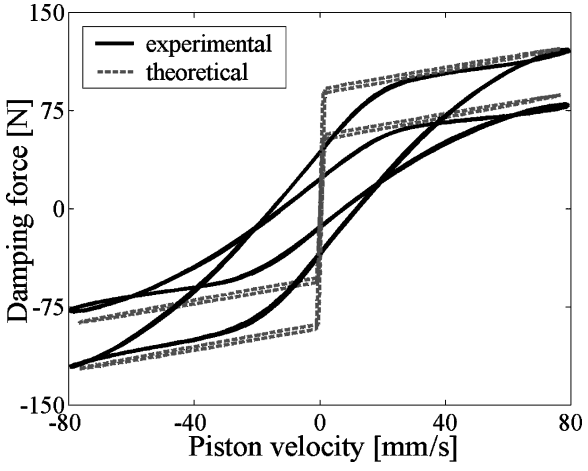

a)

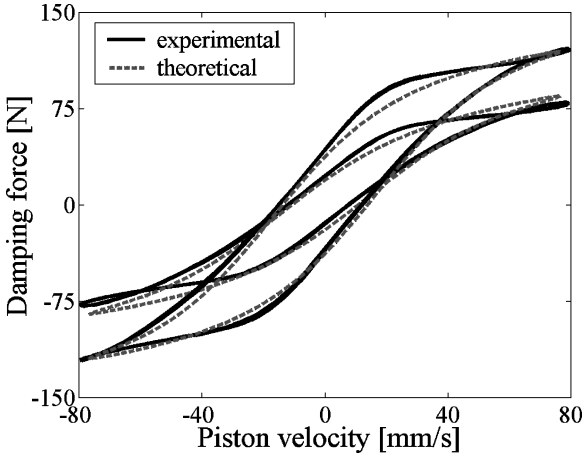

b)

Fig. 8 Damping force vs piston velocity at the different conditions (0.2 and 1.0 A at 8.5 Hz): a) Bingham-plastic model and b) nonlinear hysteresis model.

hysteresis model proposed in this study is able to capture the behavior of the MR isolator more accurately than the Bingham-plastic model.

Vibration Isolation System with MR Isolator

We now construct a vibration isolation system with the MR isolator to evaluate its controlled performances through experiment and analysis. In our analysis, the Bingham-plastic and nonlinear hysteresis models are still considered. A photograph of the experimental setup of an SDOF MR vibration isolation system is shown in Fig. 10. The MR isolator is placed between the system mass and excitation actuator. To prevent static deflection of the mass, a coil spring is installed on the MR isolator. The excitation actuator is driven by a hydraulic power system, and its excitation displacement is measured by a linear variable differential transformer (LVDT). In addition, the acceleration of the mass is measured by an accelerometer.

For theoretical analysis, the governing equation of motion of the MR vibration isolation system can be obtained as follows:

$$m\ddot{x} = -c(\dot{x} - \dot{y}) - (k + k_c)(x - y) - f_{dc} \tag{3}$$

Here, m is the system mass, k_c is the stiffness of the coil spring, x is the displacement of the mass, and y is the excitation displacement. In addition, f_{dc} is the controlled damping force, which can be expressed by

$$f_{dc} = \begin{cases} (f_{yc} + f_f)\,\mathrm{sgn}(\dot{x} - \dot{y}), & \text{for Bingham-plastic model} \\ (f_{yc} + f_f)\tanh\{[(\dot{x} - \dot{y}) \\ \quad + \lambda_1(x - y)]\lambda_2\}, & \text{for nonlinear hysteresis model} \end{cases} \tag{4}$$

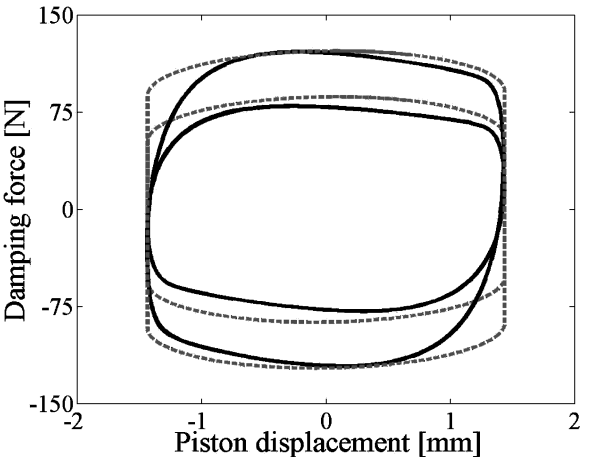

a)

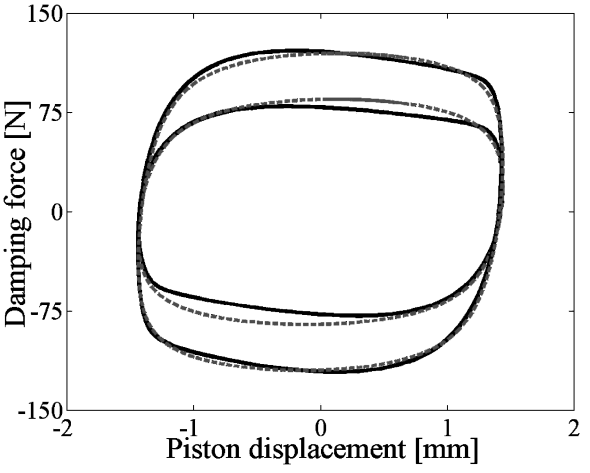

b)

Fig. 9 Damping force vs piston displacement at the different conditions (0.2 and 1.0 A at 8.5 Hz): a) Bingham-plastic model and b) nonlinear hysteresis model.

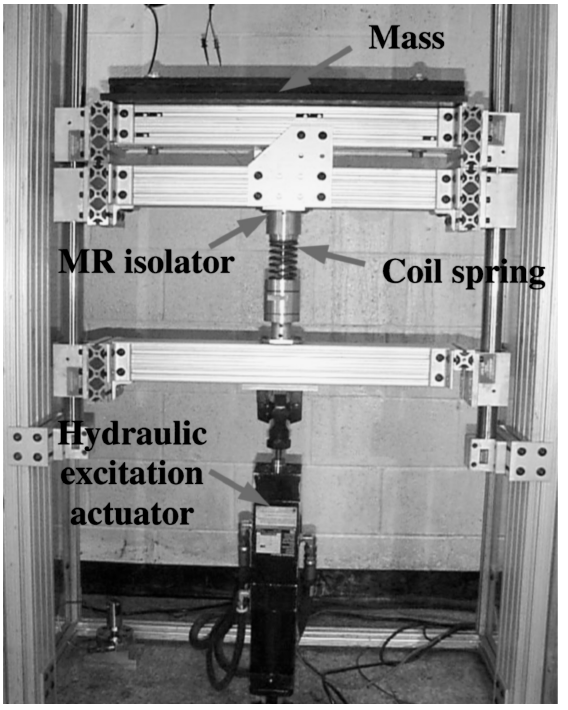

Fig. 10 Experimental setup of SDOF vibration isolation system with the MR isolator.

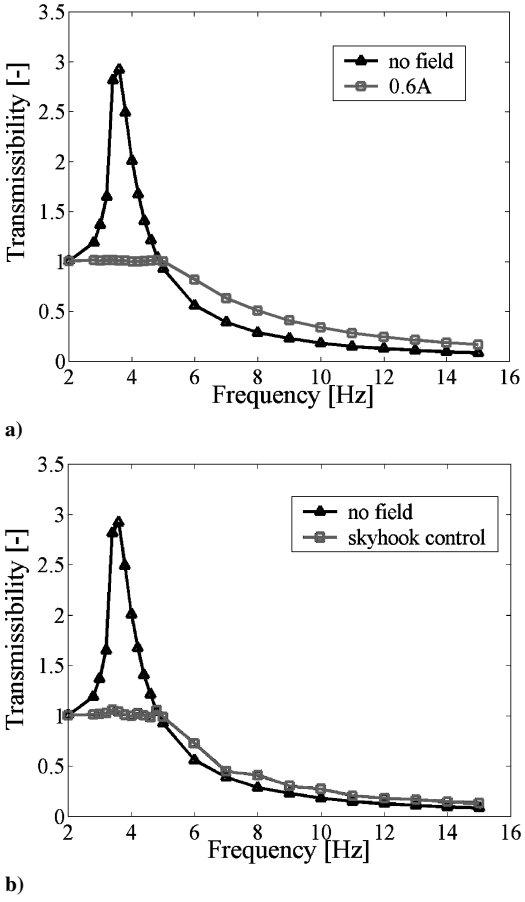

Fig. 11 Experimental results of the MR vibration isolation system in frequency domain: a) constant current input and b) skyhook control input.

Here, $f_{yc} = \alpha\, i_c^{\beta}$ is the controlled yield damping force, α and β are characteristic values of MR fluids, and i_c is the applied control current input. In this study, α and β were chosen as 80.9 and 0.38, respectively. A simple skyhook control algorithm is adopted to improve the vibration isolation performance of the MR vibration isolation system. From the simple skyhook control algorithm, the control current input is determined as follows:

$$i_c = \begin{cases} 0.54A, & \text{if} \quad \dot{x} \cdot (\dot{x} - \dot{y}) > 0 \\ 0.0A, & \text{if} \quad \dot{x} \cdot (\dot{x} - \dot{y}) \le 0 \end{cases} \tag{5}$$

Note that because the MR vibration isolation system is a semi-active-type control system, the semi-active actuation condition necessary to ensure the increment of the dissipation energy for the system was superposed in the Eq. (5) (Refs. 21 and 26–28). In this study, the system parameters are as follows: $m = 75$ kg, $c = 425$ N · s/m, $k = 1320$ N/m, and $k_c = 37{,}000$ N/m.

Control Performance

Figure 11 presents experimental results of the MR vibration isolation system under the constant current input and the simple skyhook controller in the frequency domain. The transmissibility that is computed from root-mean-square values of the acceleration of the mass and excitation, is used to predict the performance of the system. As shown in Fig. 11a, a constant current input can effectively control the vibration of the system in the resonance-only region. Particularly in the higher-frequency region above resonance frequency, constant current input deteriorates the vibration isolation performance of the system. This is because the excessive damping in the higher-frequency range has a detrimental effect on the performance of the vibration isolation system. However, from Fig. 11b, the simple skyhook control algorithm can improve the vibration isolation performance of the MR vibration isolation system at above resonance.

Figure 12 presents theoretical results of the MR vibration isolation system on the basis of the Bingham-plastic model and nonlinear

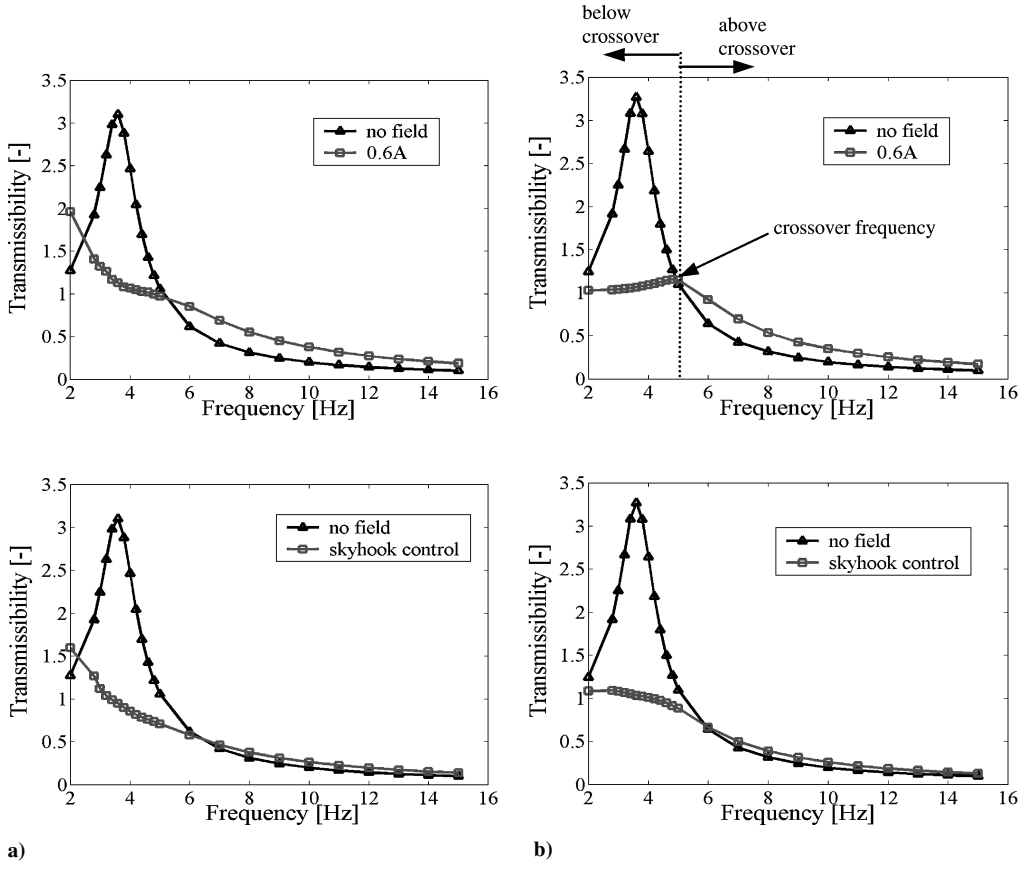

Fig. 12 Theoretical results of the MR vibration isolation system in frequency domain: a) Bingham-plastic model and b) nonlinear hysteresis model.

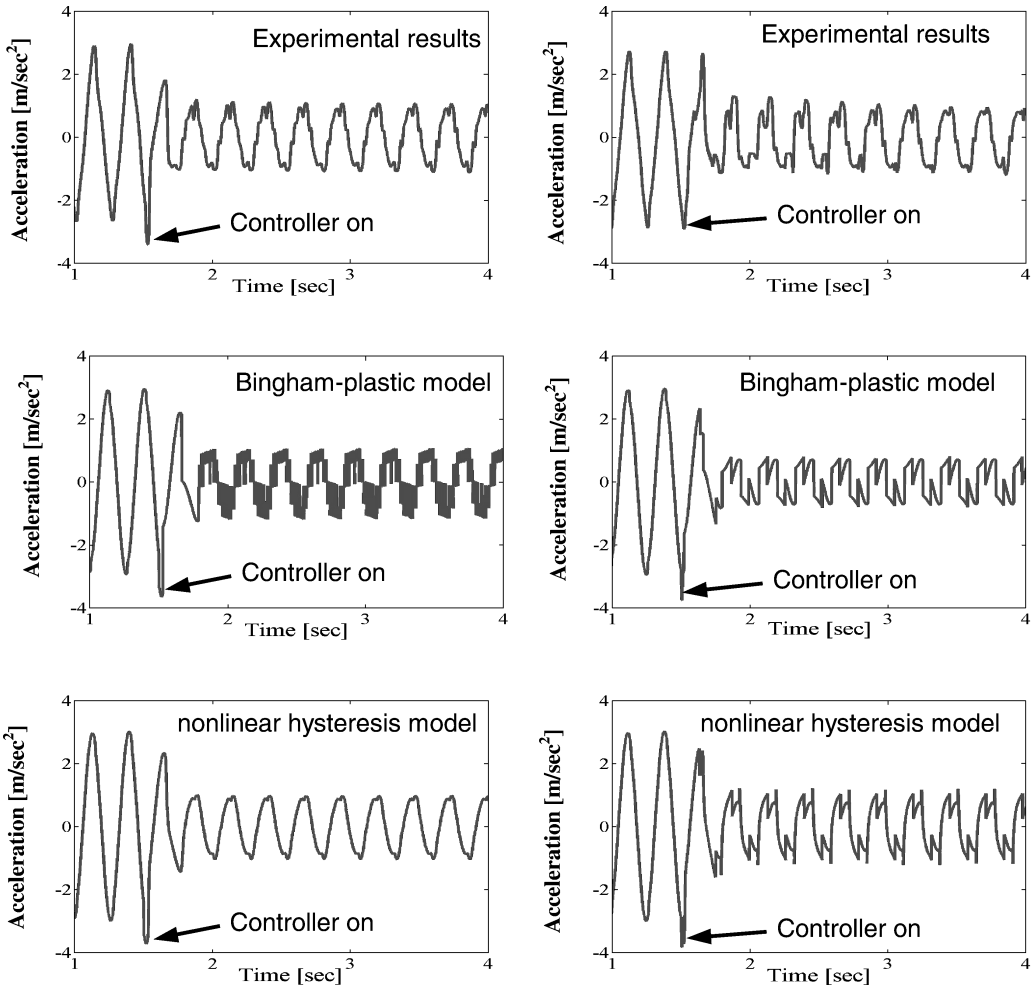

a) Constant current input b) Skyhook control input

Fig. 13 Theoretical results of the MR vibration isolation system in time domain: a) Bingham-plastic model and b) nonlinear hysteresis model.

hysteresis model in the frequency domain. Note in Fig. 12a that the Bingham-plastic model does not predict well the vibration isolation performance of the MR vibration isolation system below crossover. In contrast, although above crossover the prediction is accurate, the nonlinear hysteresis model accurately predicts the vibration isolation performance of the system both above and below crossover, as shown in Fig. 12b.

Figure 13 presents a comparison of experimental and theoretical results of the MR vibration isolation system in the time domain. Experimental and theoretical results under constant current input are shown in Fig. 13a and, for skyhook control input, results are shown in Fig. 13b. In the controllable cases, control current input is applied to the MR isolator at 1.5 s and an excitation frequency of 3.8 Hz. Note from Fig. 13 that the nonlinear hysteresis model can more accurately capture the overall behavior of the MR vibration isolation system than the Bingham-plastic model under both constant and skyhook control current inputs. In particular, noted that, in the case of the skyhook control input, the Bingham-plastic model overestimates the controlled performance of the system.

Conclusions

Experimental and theoretical analysis of a vibration isolation system that uses MR fluid-based semi-active isolators was presented under a constant and simple skyhook control algorithm. An MR vibration isolator applicable to the vibration isolation system for avionics packages was designed and manufactured in this study. To describe the practical hysteresis force characteristics of the MR isolator, a new nonlinear hysteresis model, simple in form, is proposed. The damping forces of the MR isolator with different excitation frequency and current input are measured and compared with that resulting from the hysteresis model. It was shown that the nonlinear hysteresis model could capture the force hysteresis characteristics of the MR isolator in the presence of current inputs. After that, a vibration isolation system with the MR isolator was constructed and modeled on the basis of two models, namely, the Bingham-plastic model and the nonlinear hysteresis model. Controlled performances of the MR vibration isolation system were experimentally and theoretically analyzed in the frequency and time domains. It has been demonstrated that the vibration isolation performance can be improved a great deal by the employment of the simple skyhook control algorithm, and that the nonlinear hysteresis model can accurately more predict the vibration isolation performance than the Bingham-plastic model in open- and closed-loop time and frequency domains.

Acknowledgments

This project was supported by Paulstra-Vibrachoc of Paris, France (Christian Casse, Technical Monitor). Young-Sik Jeon's visit at the University of Maryland was supported by his home institution, Yuhan College of Korea, under a visiting professorship program. This paper was given the ASME Adaptive Structures and Material Systems Best Paper Award in March 2004.

References

[1]Rivin, E. I., "Passive Engine Mounts—Some Directions for Further Development," Society of Automotive Engineers, SAE TP 850481, 1985.

[2]Singh, R., Kim, G., and Ravindra, P. V., "Linear Analysis of Automotive Hydro-Mechanical Mount with Emphasis on Decoupler Characteristics," *Journal of Sound and Vibration*, Vol. 158, No. 2, 1992, pp. 219–243.

[3]Colgate, J. E., Chang, C.-T., Chiou, Y.-C., Liu, W. K., and Keer, L. M., "Modelling of a Hydraulic Engine Mount Focusing on Response

to Sinusoidal and Composite Excitations," *Journal of Sound and Vibration*, Vol. 184, No. 3, 1995, pp. 503–528.

[4]Miller, L. R., Ahmadian, M., Nobles, C. M., and Swanson, D. A., "Modelling and Performance of An Experimental Active Vibration Isolator," *ASME Journal of Vibration and Acoustics*, Vol. 117, No. 3A, 1995, pp. 272–278.

[5]FitzSimons, P. M., and Palazzolo, J. J., "Part I: Modeling of a One-Degree-of-Freedom Active Hydraulic Mount," *ASME Journal of Dynamic Systems, Measurement, and Control*, Vol. 118, No. 3, 1996, pp. 439–442.

[6]FitzSimons, P. M., and Palazzolo, J. J., "Part II: Modeling of a One-Degree-of-Freedom Active Hydraulic Mount," *ASME Journal of Dynamic Systems, Measurement, and Control*, Vol. 118, No. 3, 1996, pp. 443–448.

[7]Ushijima, T., and Kumakawa, S., "Active Engine Mount with Piezo-Actuator for Vibration Control," Society of Automotive Engineers, SAE TP 930201, 1993.

[8]Shibayama, T., Ito, K., Gami, T., and Oku, T., "Active Engine Mount for a Large Amplitude of Idling Vibration," Society of Automotive Engineers, SAE TP 951298, 1995.

[9]Wereley, N. M., Pang, L., and Kamath, G. M., "Idealized Hysteresis Modeling of Electrorheological and Magnetorheological Dampers," *Journal of Intelligent Material Systems and Structures*, Vol. 9, No. 8, 1998, pp. 642–649.

[10]Kamath, G. M., and Wereley, N. M., "A Nonlinear Viscoelastic-Plastic Model For Electrorheological Fluids," *Smart Materials and Structures*, Vol. 6, No. 3, 1997, pp. 351–359.

[11]Kamath, G. M., Wereley, N. M., and Jolly, M. R., "Characterization of Magnetorheological Helicopter Lag Dampers," *Journal of the American Helicopter Society*, Vol. 44, No. 3, 1999, pp. 234–248.

[12]Snyder, R. A., Kamath, G. M., and Wereley, N. M., "Characterization and Analysis of Magnetorheological Damper Behavior under Sinusoidal Loading," *AIAA Journal*, Vol. 39, No. 7, 2001, pp. 1240–1253.

[13]Spencer, B. F., Jr., Dyke, S. J., Sain, M. K., and Carlson, J. D., "Phenomenological Model of a Magnetorheological Damper," *Journal of Engineering Mechanics*, Vol. 123, No. 3, 1997, pp. 230–238.

[14]Dyke, S. J., Spencer, B. F., Jr., Sain, M. K., and Carlson, J. D., "Modeling and Control of Magnetorheological Dampers for Seismic Response Reduction," *Smart Materials and Structures*, Vol. 5, No. 5, 1996, pp. 565–575.

[15]Gavin, H. P., Hanson, R. D., and Filisko, F. E., "Electrorheological Dampers, Part II: Testing and Modeling," *ASME Journal of Applied Mechanics*, Vol. 63, No. 3, 1996, pp. 676–682.

[16]Makris, N., Burton, S. A., and Taylor, D. P., "Electrorheological Damper with Annular Ducts for Seismic Protection Applications," *Smart Materials and Structures*, Vol. 5, No. 5, 1996, pp. 551–564.

[17]Sims, N. D., Stanway, R., Peel, D. J., Bullough, W. A., and Johnson, A. R., "Controllable Viscous Damping: An Experimental Study of An Electrorheological Long-Stroke Damper Under Proportional Feedback Control," *Smart Materials and Structures*, Vol. 8, No. 5, 1999, pp. 601–615.

[18]Sims, N. D., Peel, D. J., Stanway, R., Johnson, A. R., and Bullough, W. A., "The Electrorheological Long-Stroke Damper: A New Modelling Technique with Experimental Validation," *Journal of Sound and Vibration*, Vol. 229, No. 2, 2000, pp. 207–227.

[19]Choi, S. B., Lee, S. K., and Park, Y. P., "A Hysteresis Model for the Field-Dependent Damping Force of a Magnetorheological Damper," *Journal of Sound and Vibration*, Vol. 245, No. 2, 2001, pp. 375–383.

[20]Hong, S. R., Choi, S. B., Choi, Y. T., and Wereley, N. M., "Comparison of Damping Force Models for an Electrorheological Fluid Damper," *International Journal of Vehicle Design*, Vol. 33, Nos. 1–3, 2003, pp. 17–35.

[21]Karnopp, D., Crosby, M. J., and Harwood, R. A., "Vibration Control Using Semi-Active Force Generators," *ASME Journal of Engineering for Industry*, Vol. 96, No. 2, 1974, pp. 619–626.

[22]Morishita, S., and Mitsui, J., "An Electronically Controlled Engine Mount Using Electro-Rheological Fluid," Society of Automotive Engineers, SAE TP 922290, 1992.

[23]Lou, Z., Ervin, R. D., Filisko, F. E., and Winker, C. B., "An Electrorheologically Controlled Semi-Active Landing Gear," Society of Automotive Engineers, SAE TP 931403, 1993.

[24]Gavin, H. P., Hanson, R. D., and Filisko, F. E., "Electrorheological Dampers, Part I: Analysis and Design," *ASME Journal of Applied Mechanics*, Vol. 63, No. 3, 1996, pp. 669–675.

[25]Lee, H. S., and Choi, S. B., "Control and Response Characteristics of a Magneto-Rheological Fluid Damper for Passenger Vehicles," *Journal of Intelligent Material Systems and Structures*, Vol. 11, No. 1, 2000, pp. 80–87.

[26]Sturk, M., Wu, X. M., and Wong, J. Y., "Development and Evaluation of a High Voltage Supply Unit for Electrorheological Fluid Dampers," *Vehicle System Dynamics*, Vol. 24, No. 2, 1995, pp. 101–121.

[27]Wu, X., and Griffin, M. J., "A Semi-Active Control Policy to Reduce the Occurrence and Severity of End-Stop Impacts in a Suspension Seat with an Electrorheological Fluid Damper," *Journal of Sound and Vibration*, Vol. 203, No. 5, 1997, pp. 781–793.

[28]Choi, S. B., Choi, Y. T., and Jeon, Y. S., "Performance Evaluation of a Mixed Mode ER Engine Mount Via Hardware-in-the-Loop-Simulation," *Journal of Intelligent Material Systems and Structures*, Vol. 10, No. 8, 1999, pp. 671–677.